BABAR-CONF-06/013
SLAC-PUB-11978
July 2006

A measurement of CP-violation parameters in $B^0\overline{B}^0$ mixing using partially reconstructed $D^{*-}\ell^+\nu_\ell$ events at *BABAR*

The *BABAR* Collaboration

February 7, 2008

Abstract

CP violation in $B^0\overline{B}^0$ mixing is characterized by the value of the parameter $|q/p|$ being different from 1, and the Standard Model predicts this difference to be smaller than 10^{-3}. We present a measurement of this parameter using a partial reconstruction of one of the B mesons in the semileptonic channel $D^{*-}\ell^+\nu_\ell$, where only the hard lepton and the soft pion from the $D^{*-} \to \overline{D}^0\pi^-$ decay are reconstructed. The flavor of the other B is determined by means of lepton tagging. The determination of $|q/p|$ is then performed with a fit to the proper time difference of the two B decays. We use a luminosity of 200.8 fb^{-1}, collected at the $\Upsilon(4S)$ resonance by the *BABAR* detector at the PEP-II asymmetrical-energy e^+e^- collider, in the period 1999-2004. We obtain the preliminary result:

$$|q/p| - 1 = (6.5 \pm 3.4(\text{stat.}) \pm 2.0(\text{syst.})) \cdot 10^{-3}$$

Submitted to the 33$^{\text{rd}}$ International Conference on High-Energy Physics, ICHEP 06, 26 July—2 August 2006, Moscow, Russia.

Stanford Linear Accelerator Center, Stanford University, Stanford, CA 94309

Work supported in part by Department of Energy contract DE-AC03-76SF00515.

The *BABAR* Collaboration,

B. Aubert, R. Barate, M. Bona, D. Boutigny, F. Couderc, Y. Karyotakis, J. P. Lees, V. Poireau, V. Tisserand, A. Zghiche

Laboratoire de Physique des Particules, IN2P3/CNRS et Université de Savoie, F-74941 Annecy-Le-Vieux, France

E. Grauges

Universitat de Barcelona, Facultat de Fisica, Departament ECM, E-08028 Barcelona, Spain

A. Palano

Università di Bari, Dipartimento di Fisica and INFN, I-70126 Bari, Italy

J. C. Chen, N. D. Qi, G. Rong, P. Wang, Y. S. Zhu

Institute of High Energy Physics, Beijing 100039, China

G. Eigen, I. Ofte, B. Stugu

University of Bergen, Institute of Physics, N-5007 Bergen, Norway

G. S. Abrams, M. Battaglia, D. N. Brown, J. Button-Shafer, R. N. Cahn, E. Charles, M. S. Gill, Y. Groysman, R. G. Jacobsen, J. A. Kadyk, L. T. Kerth, Yu. G. Kolomensky, G. Kukartsev, G. Lynch, L. M. Mir, T. J. Orimoto, M. Pripstein, N. A. Roe, M. T. Ronan, W. A. Wenzel

Lawrence Berkeley National Laboratory and University of California, Berkeley, California 94720, USA

P. del Amo Sanchez, M. Barrett, K. E. Ford, A. J. Hart, T. J. Harrison, C. M. Hawkes, S. E. Morgan, A. T. Watson

University of Birmingham, Birmingham, B15 2TT, United Kingdom

T. Held, H. Koch, B. Lewandowski, M. Pelizaeus, K. Peters, T. Schroeder, M. Steinke

Ruhr Universität Bochum, Institut für Experimentalphysik 1, D-44780 Bochum, Germany

J. T. Boyd, J. P. Burke, W. N. Cottingham, D. Walker

University of Bristol, Bristol BS8 1TL, United Kingdom

D. J. Asgeirsson, T. Cuhadar-Donszelmann, B. G. Fulsom, C. Hearty, N. S. Knecht, T. S. Mattison, J. A. McKenna

University of British Columbia, Vancouver, British Columbia, Canada V6T 1Z1

A. Khan, P. Kyberd, M. Saleem, D. J. Sherwood, L. Teodorescu

Brunel University, Uxbridge, Middlesex UB8 3PH, United Kingdom

V. E. Blinov, A. D. Bukin, V. P. Druzhinin, V. B. Golubev, A. P. Onuchin, S. I. Serednyakov, Yu. I. Skovpen, E. P. Solodov, K. Yu Todyshev

Budker Institute of Nuclear Physics, Novosibirsk 630090, Russia

D. S. Best, M. Bondioli, M. Bruinsma, M. Chao, S. Curry, I. Eschrich, D. Kirkby, A. J. Lankford, P. Lund, M. Mandelkern, R. K. Mommsen, W. Roethel, D. P. Stoker

University of California at Irvine, Irvine, California 92697, USA

S. Abachi, C. Buchanan

University of California at Los Angeles, Los Angeles, California 90024, USA

S. D. Foulkes, J. W. Gary, O. Long, B. C. Shen, K. Wang, L. Zhang
University of California at Riverside, Riverside, California 92521, USA

H. K. Hadavand, E. J. Hill, H. P. Paar, S. Rahatlou, V. Sharma
University of California at San Diego, La Jolla, California 92093, USA

J. W. Berryhill, C. Campagnari, A. Cunha, B. Dahmes, T. M. Hong, D. Kovalskyi, J. D. Richman
University of California at Santa Barbara, Santa Barbara, California 93106, USA

T. W. Beck, A. M. Eisner, C. J. Flacco, C. A. Heusch, J. Kroseberg, W. S. Lockman, G. Nesom, T. Schalk, B. A. Schumm, A. Seiden, P. Spradlin, D. C. Williams, M. G. Wilson
University of California at Santa Cruz, Institute for Particle Physics, Santa Cruz, California 95064, USA

J. Albert, E. Chen, A. Dvoretskii, F. Fang, D. G. Hitlin, I. Narsky, T. Piatenko, F. C. Porter, A. Ryd, A. Samuel
California Institute of Technology, Pasadena, California 91125, USA

G. Mancinelli, B. T. Meadows, K. Mishra, M. D. Sokoloff
University of Cincinnati, Cincinnati, Ohio 45221, USA

F. Blanc, P. C. Bloom, S. Chen, W. T. Ford, J. F. Hirschauer, A. Kreisel, M. Nagel, U. Nauenberg, A. Olivas, W. O. Ruddick, J. G. Smith, K. A. Ulmer, S. R. Wagner, J. Zhang
University of Colorado, Boulder, Colorado 80309, USA

A. Chen, E. A. Eckhart, A. Soffer, W. H. Toki, R. J. Wilson, F. Winklmeier, Q. Zeng
Colorado State University, Fort Collins, Colorado 80523, USA

D. D. Altenburg, E. Feltresi, A. Hauke, H. Jasper, J. Merkel, A. Petzold, B. Spaan
Universität Dortmund, Institut für Physik, D-44221 Dortmund, Germany

T. Brandt, V. Klose, H. M. Lacker, W. F. Mader, R. Nogowski, J. Schubert, K. R. Schubert, R. Schwierz, J. E. Sundermann, A. Volk
Technische Universität Dresden, Institut für Kern- und Teilchenphysik, D-01062 Dresden, Germany

D. Bernard, G. R. Bonneaud, E. Latour, Ch. Thiebaux, M. Verderi
Laboratoire Leprince-Ringuet, CNRS/IN2P3, Ecole Polytechnique, F-91128 Palaiseau, France

P. J. Clark, W. Gradl, F. Muheim, S. Playfer, A. I. Robertson, Y. Xie
University of Edinburgh, Edinburgh EH9 3JZ, United Kingdom

M. Andreotti, D. Bettoni, C. Bozzi, R. Calabrese, G. Cibinetto, E. Luppi, M. Negrini, A. Petrella, L. Piemontese, E. Prencipe
Università di Ferrara, Dipartimento di Fisica and INFN, I-44100 Ferrara, Italy

F. Anulli, R. Baldini-Ferroli, A. Calcaterra, R. de Sangro, G. Finocchiaro, S. Pacetti, P. Patteri, I. M. Peruzzi,[1] M. Piccolo, M. Rama, A. Zallo
Laboratori Nazionali di Frascati dell'INFN, I-00044 Frascati, Italy

[1]Also with Università di Perugia, Dipartimento di Fisica, Perugia, Italy

A. Buzzo, R. Capra, R. Contri, M. Lo Vetere, M. M. Macri, M. R. Monge, S. Passaggio, C. Patrignani, E. Robutti, A. Santroni, S. Tosi

Università di Genova, Dipartimento di Fisica and INFN, I-16146 Genova, Italy

G. Brandenburg, K. S. Chaisanguanthum, M. Morii, J. Wu

Harvard University, Cambridge, Massachusetts 02138, USA

R. S. Dubitzky, J. Marks, S. Schenk, U. Uwer

Universität Heidelberg, Physikalisches Institut, Philosophenweg 12, D-69120 Heidelberg, Germany

D. J. Bard, W. Bhimji, D. A. Bowerman, P. D. Dauncey, U. Egede, R. L. Flack, J. A. Nash, M. B. Nikolich, W. Panduro Vazquez

Imperial College London, London, SW7 2AZ, United Kingdom

P. K. Behera, X. Chai, M. J. Charles, U. Mallik, N. T. Meyer, V. Ziegler

University of Iowa, Iowa City, Iowa 52242, USA

J. Cochran, H. B. Crawley, L. Dong, V. Eyges, W. T. Meyer, S. Prell, E. I. Rosenberg, A. E. Rubin

Iowa State University, Ames, Iowa 50011-3160, USA

A. V. Gritsan

Johns Hopkins University, Baltimore, Maryland 21218, USA

A. G. Denig, M. Fritsch, G. Schott

Universität Karlsruhe, Institut für Experimentelle Kernphysik, D-76021 Karlsruhe, Germany

N. Arnaud, M. Davier, G. Grosdidier, A. Höcker, F. Le Diberder, V. Lepeltier, A. M. Lutz, A. Oyanguren, S. Pruvot, S. Rodier, P. Roudeau, M. H. Schune, A. Stocchi, W. F. Wang, G. Wormser

Laboratoire de l'Accélérateur Linéaire, IN2P3/CNRS et Université Paris-Sud 11, Centre Scientifique d'Orsay, B.P. 34, F-91898 ORSAY Cedex, France

C. H. Cheng, D. J. Lange, D. M. Wright

Lawrence Livermore National Laboratory, Livermore, California 94550, USA

C. A. Chavez, I. J. Forster, J. R. Fry, E. Gabathuler, R. Gamet, K. A. George, D. E. Hutchcroft, D. J. Payne, K. C. Schofield, C. Touramanis

University of Liverpool, Liverpool L69 7ZE, United Kingdom

A. J. Bevan, F. Di Lodovico, W. Menges, R. Sacco

Queen Mary, University of London, E1 4NS, United Kingdom

G. Cowan, H. U. Flaecher, D. A. Hopkins, P. S. Jackson, T. R. McMahon, S. Ricciardi, F. Salvatore, A. C. Wren

University of London, Royal Holloway and Bedford New College, Egham, Surrey TW20 0EX, United Kingdom

D. N. Brown, C. L. Davis

University of Louisville, Louisville, Kentucky 40292, USA

J. Allison, N. R. Barlow, R. J. Barlow, Y. M. Chia, C. L. Edgar, G. D. Lafferty, M. T. Naisbit, J. C. Williams, J. I. Yi

University of Manchester, Manchester M13 9PL, United Kingdom

C. Chen, W. D. Hulsbergen, A. Jawahery, C. K. Lae, D. A. Roberts, G. Simi

University of Maryland, College Park, Maryland 20742, USA

G. Blaylock, C. Dallapiccola, S. S. Hertzbach, X. Li, T. B. Moore, S. Saremi, H. Staengle

University of Massachusetts, Amherst, Massachusetts 01003, USA

R. Cowan, G. Sciolla, S. J. Sekula, M. Spitznagel, F. Taylor, R. K. Yamamoto

Massachusetts Institute of Technology, Laboratory for Nuclear Science, Cambridge, Massachusetts 02139, USA

H. Kim, S. E. Mclachlin, P. M. Patel, S. H. Robertson

McGill University, Montréal, Québec, Canada H3A 2T8

A. Lazzaro, V. Lombardo, F. Palombo

Università di Milano, Dipartimento di Fisica and INFN, I-20133 Milano, Italy

J. M. Bauer, L. Cremaldi, V. Eschenburg, R. Godang, R. Kroeger, D. A. Sanders, D. J. Summers, H. W. Zhao

University of Mississippi, University, Mississippi 38677, USA

S. Brunet, D. Côté, M. Simard, P. Taras, F. B. Viaud

Université de Montréal, Physique des Particules, Montréal, Québec, Canada H3C 3J7

H. Nicholson

Mount Holyoke College, South Hadley, Massachusetts 01075, USA

N. Cavallo,[2] G. De Nardo, F. Fabozzi,[3] C. Gatto, L. Lista, D. Monorchio, P. Paolucci, D. Piccolo, C. Sciacca

Università di Napoli Federico II, Dipartimento di Scienze Fisiche and INFN, I-80126, Napoli, Italy

M. A. Baak, G. Raven, H. L. Snoek

NIKHEF, National Institute for Nuclear Physics and High Energy Physics, NL-1009 DB Amsterdam, The Netherlands

C. P. Jessop, J. M. LoSecco

University of Notre Dame, Notre Dame, Indiana 46556, USA

T. Allmendinger, G. Benelli, L. A. Corwin, K. K. Gan, K. Honscheid, D. Hufnagel, P. D. Jackson, H. Kagan, R. Kass, A. M. Rahimi, J. J. Regensburger, R. Ter-Antonyan, Q. K. Wong

Ohio State University, Columbus, Ohio 43210, USA

N. L. Blount, J. Brau, R. Frey, O. Igonkina, J. A. Kolb, M. Lu, R. Rahmat, N. B. Sinev, D. Strom, J. Strube, E. Torrence

University of Oregon, Eugene, Oregon 97403, USA

[2]Also with Università della Basilicata, Potenza, Italy
[3]Also with Università della Basilicata, Potenza, Italy

A. Gaz, M. Margoni, M. Morandin, A. Pompili, M. Posocco, M. Rotondo, F. Simonetto, R. Stroili, C. Voci

Università di Padova, Dipartimento di Fisica and INFN, I-35131 Padova, Italy

M. Benayoun, H. Briand, J. Chauveau, P. David, L. Del Buono, Ch. de la Vaissière, O. Hamon, B. L. Hartfiel, M. J. J. John, Ph. Leruste, J. Malclès, J. Ocariz, L. Roos, G. Therin

Laboratoire de Physique Nucléaire et de Hautes Energies, IN2P3/CNRS, Université Pierre et Marie Curie-Paris6, Université Denis Diderot-Paris7, F-75252 Paris, France

L. Gladney, J. Panetta

University of Pennsylvania, Philadelphia, Pennsylvania 19104, USA

M. Biasini, R. Covarelli, E. Manoni

Università di Perugia, Dipartimento di Fisica and INFN, I-06100 Perugia, Italy

C. Angelini, G. Batignani, S. Bettarini, F. Bucci, G. Calderini, M. Carpinelli, R. Cenci, F. Forti, M. A. Giorgi, A. Lusiani, G. Marchiori, M. A. Mazur, M. Morganti, N. Neri, E. Paoloni, G. Rizzo, J. J. Walsh

Università di Pisa, Dipartimento di Fisica, Scuola Normale Superiore and INFN, I-56127 Pisa, Italy

M. Haire, D. Judd, D. E. Wagoner

Prairie View A&M University, Prairie View, Texas 77446, USA

J. Biesiada, N. Danielson, P. Elmer, Y. P. Lau, C. Lu, J. Olsen, A. J. S. Smith, A. V. Telnov

Princeton University, Princeton, New Jersey 08544, USA

F. Bellini, G. Cavoto, A. D'Orazio, D. del Re, E. Di Marco, R. Faccini, F. Ferrarotto, F. Ferroni, M. Gaspero, L. Li Gioi, M. A. Mazzoni, S. Morganti, G. Piredda, F. Polci, F. Safai Tehrani, C. Voena

Università di Roma La Sapienza, Dipartimento di Fisica and INFN, I-00185 Roma, Italy

M. Ebert, H. Schröder, R. Waldi

Universität Rostock, D-18051 Rostock, Germany

T. Adye, N. De Groot, B. Franek, E. O. Olaiya, F. F. Wilson

Rutherford Appleton Laboratory, Chilton, Didcot, Oxon, OX11 0QX, United Kingdom

R. Aleksan, S. Emery, A. Gaidot, S. F. Ganzhur, G. Hamel de Monchenault, W. Kozanecki, M. Legendre, G. Vasseur, Ch. Yèche, M. Zito

DSM/Dapnia, CEA/Saclay, F-91191 Gif-sur-Yvette, France

X. R. Chen, H. Liu, W. Park, M. V. Purohit, J. R. Wilson

University of South Carolina, Columbia, South Carolina 29208, USA

M. T. Allen, D. Aston, R. Bartoldus, P. Bechtle, N. Berger, R. Claus, J. P. Coleman, M. R. Convery, M. Cristinziani, J. C. Dingfelder, J. Dorfan, G. P. Dubois-Felsmann, D. Dujmic, W. Dunwoodie, R. C. Field, T. Glanzman, S. J. Gowdy, M. T. Graham, P. Grenier,[4] V. Halyo, C. Hast, T. Hryn'ova, W. R. Innes, M. H. Kelsey, P. Kim, D. W. G. S. Leith, S. Li, S. Luitz, V. Luth, H. L. Lynch, D. B. MacFarlane, H. Marsiske, R. Messner, D. R. Muller, C. P. O'Grady, V. E. Ozcan, A. Perazzo, M. Perl, T. Pulliam, B. N. Ratcliff, A. Roodman, A. A. Salnikov, R. H. Schindler, J. Schwiening, A. Snyder, J. Stelzer, D. Su, M. K. Sullivan, K. Suzuki, S. K. Swain, J. M. Thompson, J. Va'vra, N. van

[4]Also at Laboratoire de Physique Corpusculaire, Clermont-Ferrand, France

Bakel, M. Weaver, A. J. R. Weinstein, W. J. Wisniewski, M. Wittgen, D. H. Wright, A. K. Yarritu, K. Yi, C. C. Young

Stanford Linear Accelerator Center, Stanford, California 94309, USA

P. R. Burchat, A. J. Edwards, S. A. Majewski, B. A. Petersen, C. Roat, L. Wilden

Stanford University, Stanford, California 94305-4060, USA

S. Ahmed, M. S. Alam, R. Bula, J. A. Ernst, V. Jain, B. Pan, M. A. Saeed, F. R. Wappler, S. B. Zain

State University of New York, Albany, New York 12222, USA

W. Bugg, M. Krishnamurthy, S. M. Spanier

University of Tennessee, Knoxville, Tennessee 37996, USA

R. Eckmann, J. L. Ritchie, A. Satpathy, C. J. Schilling, R. F. Schwitters

University of Texas at Austin, Austin, Texas 78712, USA

J. M. Izen, X. C. Lou, S. Ye

University of Texas at Dallas, Richardson, Texas 75083, USA

F. Bianchi, F. Gallo, D. Gamba

Università di Torino, Dipartimento di Fisica Sperimentale and INFN, I-10125 Torino, Italy

M. Bomben, L. Bosisio, C. Cartaro, F. Cossutti, G. Della Ricca, S. Dittongo, L. Lanceri, L. Vitale

Università di Trieste, Dipartimento di Fisica and INFN, I-34127 Trieste, Italy

V. Azzolini, N. Lopez-March, F. Martinez-Vidal

IFIC, Universitat de Valencia-CSIC, E-46071 Valencia, Spain

Sw. Banerjee, B. Bhuyan, C. M. Brown, D. Fortin, K. Hamano, R. Kowalewski, I. M. Nugent, J. M. Roney, R. J. Sobie

University of Victoria, Victoria, British Columbia, Canada V8W 3P6

J. J. Back, P. F. Harrison, T. E. Latham, G. B. Mohanty, M. Pappagallo

Department of Physics, University of Warwick, Coventry CV4 7AL, United Kingdom

H. R. Band, X. Chen, B. Cheng, S. Dasu, M. Datta, K. T. Flood, J. J. Hollar, P. E. Kutter, B. Mellado, A. Mihalyi, Y. Pan, M. Pierini, R. Prepost, S. L. Wu, Z. Yu

University of Wisconsin, Madison, Wisconsin 53706, USA

H. Neal

Yale University, New Haven, Connecticut 06511, USA

1 INTRODUCTION

Although CP violation has been established both in the interference between decay and mixing and in direct B decay, CP violation in the mixing alone has up to now eluded experimental observation.

In the standard mixing formalism, the effective Hamiltonian is expressed as the sum of a mass and a decay matrix ($\mathbf{H} = \mathbf{M} - i/2\ \mathbf{\Gamma}$) and the B mass eigenstates are connected to the flavor eigenstates by:

$$\begin{aligned} |B_L\rangle &= p|B^0\rangle + q|\overline{B}^0\rangle \\ |B_H\rangle &= p|B^0\rangle - q|\overline{B}^0\rangle. \end{aligned} \tag{1}$$

The absolute value of the ratio q/p can be written in this notation as:

$$\left|\frac{q}{p}\right|^2 = \left|\sqrt{\frac{M_{12}^* - i/2\ \Gamma_{12}^*}{M_{12} - i/2\ \Gamma_{12}}}\right|^2 \simeq 1 - \mathrm{Im}\left(\frac{\Gamma_{12}}{M_{12}}\right) \tag{2}$$

so it is exactly equal to 1 in a CP-conserving scenario (where the off-diagonal elements of the mass and decay matrices are real, that is $M_{12} = M_{12}^*$, $\Gamma_{12} = \Gamma_{12}^*$), while it differs by a small quantity if CP is violated in mixing. The current theoretical predictions on this quantity in the Standard Model (SM) are $2 \cdot 10^{-4} \lesssim |q/p| - 1 \lesssim 6 \cdot 10^{-4}$ [1, 2].

However, recent theoretical publications [3] have pointed out that in some New Physics (NP) general scenarios, the predictions for this quantity can be significantly different with respect to the SM. Making only the assumptions that the CKM [4] is a 3×3 unitary matrix, and the tree-level processes are dominated by the SM, the matrix element M_{12} in this scenario can be related to the SM one by the formula:

$$M_{12}^{\mathrm{NP}} = r_d^2 e^{2i\theta_d} M_{12}^{\mathrm{SM}} \tag{3}$$

where r_d and θ_d are general New Physics amplitude and phase, while Γ_{12} is not modified. The CP asymmetry in mixing can be written as:

$$\begin{aligned} A_{SL} &= \frac{\Gamma(\overline{B}^0 \to \ell^+ X) - \Gamma(B^0 \to \ell^- X)}{\Gamma(\overline{B}^0 \to \ell^+ X) + \Gamma(B^0 \to \ell^- X)} \simeq \\ &\simeq 2(1 - |q/p|) = -\mathrm{Re}\left(\frac{\Gamma_{12}}{M_{12}}\right)^{\mathrm{SM}} \frac{\sin 2\theta_d}{r_d^2} + \mathrm{Im}\left(\frac{\Gamma_{12}}{M_{12}}\right)^{\mathrm{SM}} \frac{\cos 2\theta_d}{r_d^2} \end{aligned} \tag{4}$$

If the New Physics phase is significantly different from 0, the real part of Γ_{12}/M_{12} can become dominant, enhancing the asymmetry up to an order of magnitude. Together with the measurements of CKM parameters, an accurate determination of $|q/p|$ is therefore an additional constraint on New Physics models.

Measurements of $|q/p|$ at the B-factories are performed both using inclusive dilepton events [5, 6] or B mesons fully reconstructed into flavor or CP eigenstates [7]. The most precise result obtained up to now from the inclusive dilepton method is $|q/p| - 1 = (-0.8 \pm 2.7 \pm 1.9) \cdot 10^{-3}$ [6], where the first uncertainty is statistical, the second systematic. Analogous techniques have also been used by the D$\emptyset$ experiment at the Tevatron [8]: the measured parameter in this analysis is not a determination of $|q/p|$ alone, but also involves contributions from the CP violation in B_s mixing [9], and this has allowed to set constraints also on New Physics in the B_s sector.

In this analysis we exploit the partial reconstruction of $B^0 \to D^{*-}\ell^+\nu_\ell$ events. Though the total statistics is not as high as in the dilepton case, we can keep the charged B background at

a lower level, while selecting a greater number of events than in an analysis requiring the full reconstruction of a hadronic or semileptonic decay as a tag for the B flavor. At the same time, since the reconstructed and tag side are well defined, a procedure to determine particle detection asymmetries from data (explained in Sec. 4) can be carried out. In this way, we do not need dedicated control samples to determine the asymmetry induced by the experimental cuts.

2 THE *BABAR* DETECTOR AND DATASET

The data used in this analysis were collected with the *BABAR* detector at the PEP-II asymmetrical-energy e^+e^- storage ring in the period 1999-2004; they correspond to an integrated luminosity of 200.8 fb^{-1} (i.e. about 110 million $B^0\overline{B}^0$ pairs) taken at the mass of the $\Upsilon(4S)$ resonance ($\sqrt{s}$ = 10.58 GeV), plus 21.6 fb^{-1} taken about 40 MeV below. Samples of simulated $\Upsilon(4S) \to B^0\overline{B}^0$ and B^+B^- events are used to estimate efficiencies, study background and detector asymmetries.

The *BABAR* detector is described in detail elsewhere [10]. Tracking of charged particles is provided by a five-layer silicon vertex tracker (SVT) and a 40-layer drift chamber (DCH). Vertices and soft pion tracks are mainly reconstructed using information from the SVT. Cherenkov radiation detected in a ring-imaging detector (DIRC) is used for particle identification. An electromagnetic calorimeter (EMC), which consists of 6580 thallium-doped CsI crystals, is used to measure electron energies. These systems are mounted inside a 1.5 T solenoidal superconducting magnet. The flux return of the magnet (IFR) is equipped with Resistive Plate Chambers providing muon identification.

3 SELECTION METHOD AND SAMPLE COMPOSITION

The decay rates for neutral B mesons can be calculated theoretically as a function of Δt, the time difference between the decays of the two B^0 mesons, taking into account both the time evolution of the mass eigenstates and the fact that they are produced coherently from the $\Upsilon(4S)$ resonance. We approximate $\Delta t \sim \Delta z/(\langle\beta\gamma\rangle c)$, where Δz is the measured distance between the decay vertices projected along the beam direction (z axis) and $\langle\beta\gamma\rangle$ is the average boost of the $\Upsilon(4S)$ in the laboratory frame. The method used to determine $|q/p|$ is a two-dimensional fit to the set of variables (Δt, $\sigma_{\Delta t}$) with a binned extended maximum likelihood approach, where $\sigma_{\Delta t}$ is the per-event error calculated on Δt.

To discriminate events with a $B\overline{B}$ pair from events which originate from the production of light quarks, we require the ratio of the second to the zeroth Fox-Wolfram moment [11] $R_2 < 0.5$. The total number of charged tracks in the event is required to be greater than 4, to discard lepton pair production. We also calculate the invariant mass of the two highest-momentum leptons in the event and we apply a veto on the regions $M_{ll} < 0.35$ GeV/c^2 (converted photon rejection) and $3.07 < M_{ll} < 3.14$ GeV/c^2 (J/ψ rejection).

Different techniques are then used to identify the two B mesons in an event. For the first ($B_{\rm rec}$) we select $B^0 \to D^{*-}\ell^+\nu_\ell$ events with partial reconstruction of the decay $D^{*-} \to \overline{D}^0\pi_s^-$, using only the charged lepton from the B^0 decay and the soft pion (π_s^-) from the D^{*-} decay. The $\overline{D}^0$ decay is not reconstructed, resulting in high selection efficiency. Electrons are identified using dE/dx measurements in the DCH, the DIRC information and the ratio between the energy deposited in the EMC crystals and the measured momentum in the DCH. Muons are identified using the dE/dx measurements in the DCH, the DIRC information and the number of hits in the IFR. Due to the limited phase space available in the D^* decay, the π_s is emitted within a cone with

a half-opening-angle of approximately one radian and centered about the D^* motion direction [12]. We approximate the direction of the D^* to be that of the π_s and estimate the energy $\tilde{E}_{D^*}$ of the D^* as a linear function of the energy of the π_s, with parameters taken from the simulation. We define the square of the missing neutrino mass as:

$$M_\nu^2 = \left(\frac{\sqrt{s}}{2} - \tilde{E}_{D^*} - E_\ell\right)^2 - (\tilde{\mathbf{p}}_{D^*} + \mathbf{p}_\ell)^2, \tag{5}$$

where all quantities are defined in the $\Upsilon(4S)$ frame. We neglect the momentum of the B^0 (approximately 0.34 GeV/c), and identify the B^0 energy with half the total energy of the events ($\sqrt{s}/2$). E_ℓ and $\mathbf{p}_\ell$ are the energy and momentum vector of the lepton and $\tilde{\mathbf{p}}_{D^*}$ is the estimated momentum vector of the D^*. The distribution of M_ν^2 is peaked for signal events, while it is spread over a wide range for background events.

We determine the B^0 decay point from a vertex fit of the ℓ and π_s tracks, constrained to the beam-spot position in the plane perpendicular to the beam axis (the x-y plane). The beam spot position and size are determined on a run-by-run basis using two-prong events [10]. Its size in the horizontal (x) direction is on average 120 μm. Although the beam spot size in the vertical (y) direction is only 5.6 μm, we use a constraint of 50 μm in the vertex fit to account for the flight distance of the B^0 in the x-y plane.

To suppress leptons from charm meson decays, we use only high-momentum leptons in the range $1.3 < p_\ell < 2.4$ GeV/c. The π_s candidates have momenta (p_{π_s}) between 60 and 200 MeV/c. We reject events for which the χ^2 probability of the vertex fit, $\mathcal{P}_V$, is less than 0.1%. We do not use dedicated optimization procedures for these cuts, rather we apply a selection criterion to a likelihood ratio, $\mathcal{X}$, calculated from the signal and background distributions of p_ℓ, p_{π_s}, and $\mathcal{P}_V$. We reject events for which $\mathcal{X}$ is lower than 0.3 and we retain the $\ell - \pi_s$ pair with the highest value of $\mathcal{X}$ when more than one candidate is found.

The flavor of the other B meson ($B_{\rm tag}$) is determined by means of lepton tagging ($\ell = e,\ \mu$). A cut on the momentum in the center-of-mass frame is applied: $1.0 < p_\ell < 2.35$ ($1.1 < p_\ell < 2.35$) GeV/c for electrons (muons). If more than one lepton track in an event survives, the one with the largest momentum is used to determine the flavor of the $B_{\rm tag}$. The track selected for tagging is used to compute the tag vertex position, using a procedure analogous to that described above. We finally require $|\Delta z| < 3$ mm and $0 < \sigma_{\Delta z} < 0.5$ mm.

These selection criteria accept 470,877 events in the data sample, which we will refer to as *tagged* events, and 5,291,868 partially reconstructed events that fail only the requirements of lepton tagging, which we will refer to as *untagged* events, and to B^0 untagged if the $B_{\rm rec}$ is reconstructed as a B^0 and $\overline{B}^0$ untagged if the $B_{\rm rec}$ is reconstructed as a $\overline{B}^0$. Fig. 1 shows the distributions of the squared neutrino mass for tagged, B^0 untagged and $\overline{B}^0$ untagged events. Different components are recognized in the total sample: *signal* events, due to $D^{*-}\ell^+\nu_\ell$ events, including the radiative decays $D^{*-}\ell^+\nu_\ell\ \gamma/\pi^0$ and other decays with the same final signature, like $B^0 \to D^*\tau/X_c$ ($\tau/X_c \to \ell X$); *peaking* background events, that correspond to decays of charged B mesons which peak in the M_ν^2 distribution, as the signal, like $B^+ \to D^{**0}\ell^+\nu_\ell$, $D^{**0} \to D^{*-}\pi^+$; *combinatorial* events, corresponding to all $B\overline{B}$ decays not included in the previous categories; *continuum* events, coming from light quark decays $e^+e^- \to q\bar{q}$ with $q = u, d, c, s$ or $e^+e^- \to \ell^+\ell^-$ with $\ell = e, \mu, \tau$.

The following procedure is used to determine the fractions of the various components in data. The M_ν^2 distributions are fitted separately for the different types of events, using Monte Carlo events for the $B\overline{B}$ components and off-resonance events for the continuum component. The probability density functions (PDFs) for the different components are a Gaussian plus a function $\mathcal{B}(M_\nu^2)$ [13]

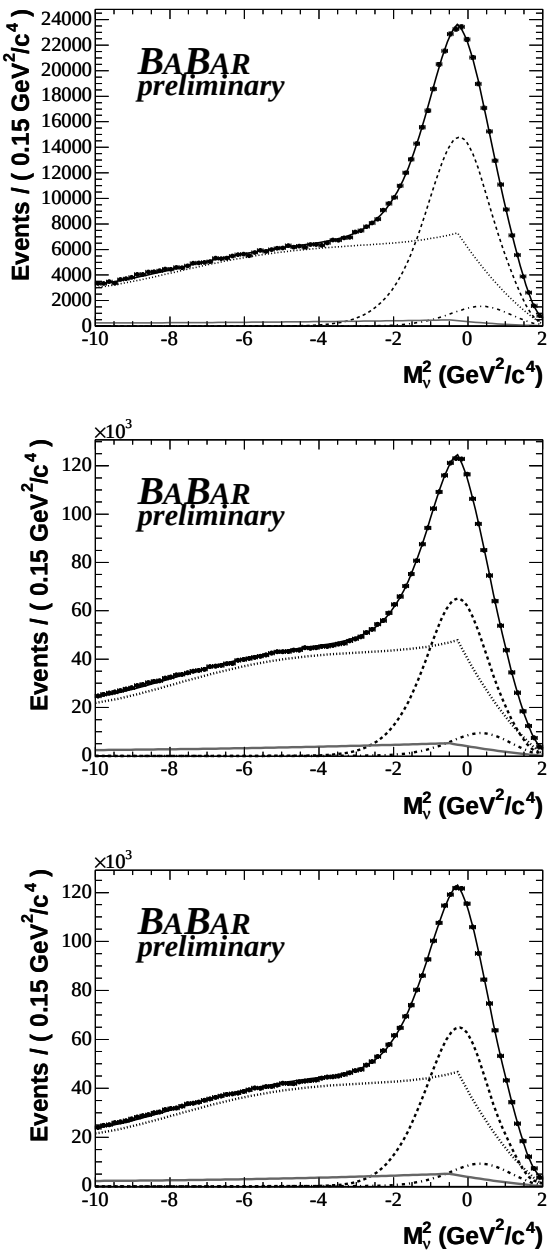

Figure 1: Squared neutrino mass distributions for the tagged (top), B^0 untagged (center) and $\overline{B}^0$ untagged (bottom) data events. The following fitted contributions are superimposed: continuum (solid grey line), combinatorial (dotted), $B^{\pm}$ peaking (dash-dotted), signal (dashed), all (solid black).

for signal and peaking background, and piecewise continuous polynomials for combinatorial and continuum samples. For signal events, we find the distribution peaking slightly below zero mainly because of soft pion decays in flight and electron energy losses; as for the peaking background, the shift to larger positive values is due to the fact that in this case we neglect the presence of one (or more) additional particles. We then fit the data sample, fixing all the shape parameters for peaking, combinatorial and continuum background. The fraction of continuum $f^{\rm cont}$ is also fixed, using the ratio between on-resonance and off-resonance luminosities, as well as the fraction of peaking background $f^{\rm peak}$, that is extracted from the fit on Monte Carlo. Conversely we float the signal shape parameters and the fraction of signal $f^{\rm sig}$, determining also the fraction of combinatorial background $f^{\rm comb} = 1 - f^{\rm sig} - f^{\rm peak} - f^{\rm cont}$.

The fractions determined with this procedure are summarized in Table 1 for the different data samples. The M_ν^2 region $-4.0 < M_\nu^2 < 2.0$ GeV$^2/c^4$ is defined as *signal region* and will be used in the nominal fits from now on. The remaining part ($-10.0 < M_\nu^2 < -4.0$ GeV$^2/c^4$) will be referred to as *side-band region* and will be used in some fits to Δt to determine combinatorial background parameters. Table 1 also shows fractions extrapolated to the signal region only.

Table 1: Fractions of signal, continuum, peaking and combinatorial background, extracted from M_ν^2 fits for the tagged, B^0 untagged and $\overline{B}^0$ untagged samples. The first uncertainties refer to the statistical uncertainty from the fit, the second are systematic errors from the shape parameter fixing.

Sample	Parameter	Fraction in the whole M_ν^2 region	Fraction extrapolated to the signal region
Tagged	$f^{\rm sig}$	$(32.72 \pm 0.15 \pm 0.58)\%$	$(46.59 \pm 0.21 \pm 0.82)\%$
	$f^{\rm peak}$	4.03%	5.54%
	$f^{\rm cont}$	4.12%	3.14%
	$f^{\rm comb}$	$(59.13 \pm 0.15 \pm 0.58)\%$	$(44.73 \pm 0.21 \pm 0.82)\%$
Untagged +	$f^{\rm sig}$	$(23.51 \pm 0.03 \pm 0.27)\%$	$(35.72 \pm 0.05 \pm 0.41)\%$
	$f^{\rm peak}$	3.05%	4.47%
	$f^{\rm cont}$	6.47%	5.38%
	$f^{\rm comb}$	$(66.97 \pm 0.03 \pm 0.27)\%$	$(54.43 \pm 0.05 \pm 0.41)\%$
Untagged −	$f^{\rm sig}$	$(24.23 \pm 0.04 \pm 0.20)\%$	$(36.33 \pm 0.06 \pm 0.30)\%$
	$f^{\rm peak}$	3.02%	4.42%
	$f^{\rm cont}$	6.14%	5.20%
	$f^{\rm comb}$	$(66.61 \pm 0.04 \pm 0.20)\%$	$(54.05 \pm 0.06 \pm 0.30)\%$

4 TIME-DEPENDENT ANALYSIS

Since the B^0 mesons can undergo oscillation, we will refer to *mixed* events when both decay in the same flavor state (B^0B^0 or $\overline{B}^0\overline{B}^0$), and define the mixing state $s_m = -1$ for such events. Conversely, we will refer to *unmixed* events ($s_m = 1$) if the flavors of the two B mesons are opposite. Similarly we define $s_t = 1$ if the $B_{\rm tag}$ is a B^0, $s_t = -1$ if the $B_{\rm tag}$ is a $\overline{B}^0$.

The calculation of the decay rate for the four tag-mixing states is straightforward, since we are dealing with semileptonic B^0 decays both on the reconstructed and tag side and these are pure

flavor eigenstates:

$$s_m = -1: \qquad \mathcal{F}(\Delta t) = \frac{1}{2\tau_{B^0}} e^{-\frac{|\Delta t|}{\tau_{B^0}}} \left|\frac{q}{p}\right|^{-2s_t} [1 - \cos(\Delta m_d \Delta t)]$$
$$s_m = 1: \qquad \mathcal{F}(\Delta t) = \frac{1}{2\tau_{B^0}} e^{-\frac{|\Delta t|}{\tau_{B^0}}} [1 + \cos(\Delta m_d \Delta t)] \tag{6}$$

where Δm_d is the B^0 oscillation frequency, τ_{B^0} is the average lifetime of the physical states and we set $\Delta\Gamma$, the lifetime difference between the physical states, equal to 0.

For the Δt distribution of signal events we use Eq. (6), modified to account for several experimental effects.

The B-tagging algorithm introduces a modification to the theoretical PDFs as there is a finite probability per event (called the *mistag rate*) of falsely tagging with a wrong-sign lepton candidate. Considering a B^0 mistag rate (i.e. the probability for a true B^0 being tagged as a $\overline{B}^0$) and a $\overline{B}^0$ mistag rate (i.e. the probability for a true $\overline{B}^0$ being tagged as a B^0), we define w as the average value of these probabilities and Δw as their difference. Also, the signal PDFs are modified to reflect the fact that reconstruction efficiency for $\ell^+\pi_s^-$ pairs can be different from the reconstruction efficiency for $\ell^-\pi_s^+$ pairs. We therefore define an average reconstruction efficiency ε_{rec} and a *reconstruction asymmetry* A_{rec}. In the same way, the tagging efficiency for positive leptons can be different from the tagging efficiency for negative leptons, so we define an average tagging efficiency ε_{tag} and a *tagging asymmetry* A_{tag}. We normalize our distributions to an average reconstruction efficiency $\varepsilon_{rec} = 1$.

To account for the finite resolution of vertex determinations, the function of the true lifetime difference Δt_{true} must be convolved with a decay time difference resolution function. We adopt a 3-Gaussian description where the two main contributions (referred to as "narrow" and "wide") depend on the per-event error of the vertex separation, $\sigma_{\Delta t}$, while the third ("outlier" Gaussian) is independent of $\sigma_{\Delta t}$:

$$\mathcal{R}(b_n, s_n, b_w, s_w, s_o, f_w, f_o) = f_o \frac{1}{\sqrt{2\pi} s_o} e^{-\frac{t^2}{2s_o^2}} +$$
$$+ f_w \frac{1}{\sqrt{2\pi} s_w \sigma_{\Delta t}} e^{-\frac{(t - b_w\sigma_{\Delta t})^2}{2(s_w\sigma_{\Delta t})^2}} + (1 - f_w - f_o) \frac{1}{\sqrt{2\pi} s_n \sigma_{\Delta t}} e^{-\frac{(t - b_n\sigma_{\Delta t})^2}{2(s_n\sigma_{\Delta t})^2}} \tag{7}$$

where $t \equiv \Delta t - \Delta t_{true}$, b_i and s_i $(i = n, w)$ are respectively the biases and the error scale factors for the narrow and wide components, while s_o is the standard deviation of the outlier Gaussian (for this component we assume $b_o = 0$); f_w and f_o are respectively the fractions of wide and outlier Gaussians.

Accounting for these effects, we define a PDF for signal events and *direct* leptons, meaning tagging leptons that do not originate from secondary charmed meson decay:

$$\mathcal{F}^{\rm sig}_{\rm dir}(\Delta t, \sigma_{\Delta t} | s_m, s_t) = \mathcal{F}^{meas}(\Delta t, \sigma_{\Delta t} | s_m, s_t) \otimes \mathcal{R}^{\rm sig}_{\rm dir} \tag{8}$$

where, using the definition $k = |q/p| - 1$:

$$s_m = -1: \qquad \mathcal{F}^{\rm meas}(\Delta t) = \frac{\varepsilon_{tag}}{4\tau_{B^0}} (1 + s_t A_{rec}) e^{-\frac{|\Delta t|}{\tau_{B^0}}} \{[1 - s_t(\Delta w + 2k(1-w) - A_{tag}(1-2w))]$$
$$-[1 - 2w + s_t(A_{tag} - 2k(1-w))] \cos(\Delta m_d \Delta t)\} \tag{9}$$

$$s_m = 1: \qquad \mathcal{F}^{\rm meas}(\Delta t) = \frac{\varepsilon_{tag}}{4\tau_{B^0}}(1 - s_t A_{rec}) e^{-\frac{|\Delta t|}{\tau_{B^0}}} \{[1 - s_t(\Delta w - 2kw - A_{tag}(1-2w))] + [1 - 2w + s_t(A_{tag} + 2kw)]\cos(\Delta m_d \Delta t)\} \tag{10}$$

For signal events in which the tagging lepton comes from a secondary charm decay (*cascade* leptons), we use different PDFs according to the two possibilities that the charm meson is a product of the $B_{\rm tag}$ or is the unreconstructed $\overline{D}^0$ on the decay side (*decay-side tagged* events). In the former case we just take the signal PDFs with the reversed tag information: $\mathcal{F}^{\rm sig}_{\rm cas}(\Delta t, \sigma_{\Delta t}|s_m, s_t) = \mathcal{F}^{\rm sig}_{\rm dir}(\Delta t, \sigma_{\Delta t}| - s_m, -s_t)$ and we allow for different mistag and resolution parameters. In the latter case, we use a simple exponential term:

$$\mathcal{F}_{\rm Dtag}(\Delta t, \sigma_{\Delta t}|s_m, s_t) = \frac{1}{2\tau_{D_e}} e^{-\frac{|\Delta t|}{\tau_{D_e}}}(1 + s_m D_{\rm Dtag})(1 + s_t A'_{tag})(1 - s_t s_m A_{rec}) \otimes \mathcal{R}_{\rm Dtag} \tag{11}$$

where τ_{D_e} is an effective D^0 lifetime and A'_{tag} is a distinct tagging asymmetry for this sample (see Sec. 5). We characterize from now on the mistag in a given sample j in terms of the *dilution* parameter $D_j = 1 - 2w_j$.

For charged B peaking background events, we similarly use a pure lifetime PDF for the direct component:

$$\mathcal{F}^{+}_{\rm dir}(\Delta t, \sigma_{\Delta t}|s_m, s_t) = \frac{1}{2\tau_{B^+}} e^{-\frac{|\Delta t|}{\tau_{B^+}}}(1 + s_m D_+)(1 + s_t A_{tag})(1 - s_t s_m A_{rec}) \otimes \mathcal{R}^{\rm sig}_{\rm dir} \tag{12}$$

while we use Eq. (11) for the decay-side tagged events.

For combinatorial background events, we recognize different components that can be parameterized with the PDFs defined above, but with sets of effective parameters that need to be determined from the M^2_ν sidebands. For the neutral part we take into account three contributions: first, the events in which both leptons in the events originate directly from the two B mesons, even if the reconstructed side is not a genuine $D^{*-}\ell^+\nu_\ell$ event. For example, these may be other semileptonic B decays in which the reconstructed soft pion candidate is actually a random track in the event. For these events we use Eqs. (9) and (10), where some shape parameters are allowed to differ from the corresponding ones for signal, since the vertex position is mis-determined using a wrong pion track. We also allow $A^{\rm bkg}_{rec}$ to be distinct from $A^{\rm dir}_{rec}$ for the same reason, but we use the same CP asymmetry parameterization of the signal, since this kind of events carries the correct tag-mixing information. Second, the same procedure applies to cascade combinatorial events. The third contribution comes from events in which the tag track is coming directly from a B, while the lepton on the decay side comes from a secondary charm meson. For this kind of events we assume: $\mathcal{F}^{\rm bkg}_{\rm cas,2}(\Delta t, \sigma_{\Delta t}|s_m, s_t) = \mathcal{F}^{\rm bkg}_{\rm dir}(\Delta t, \sigma_{\Delta t}| - s_m, s_t)$ and we allow for different mistag and resolution parameters with respect to the direct lepton case. For decay-side tagged and charged B events the descriptions of Eqs. (11) and (12) apply also for combinatorial events, given the changes of parameterization for resolution and asymmetries.

For continuum events we use a single lifetime distribution:

$$\mathcal{F}^{\rm cont}(\Delta t, \sigma_{\Delta t}|s_m, s_t) = \frac{1}{2\tau_{\rm cont}} e^{-\frac{|\Delta t|}{\tau_{\rm cont}}}(1 + s_m D_{\rm cont})(1 + s_t A^{\rm cont}_{tag})(1 - s_t s_m A^{\rm cont}_{rec}) \otimes \mathcal{R}^{\rm bkg}_{\rm dir} \tag{13}$$

Its parameters are all determined from a fit to off-resonance events.

In summary, the Δt total PDF will be a sum of all the terms so far introduced:

$$\begin{aligned}
&\mathcal{F}(\Delta t, \sigma_{\Delta t}|s_m, s_t) = \\
&f^{\rm sig}\{(1-g^{\rm sig}_{\rm Dtag})[(1-g^{\rm sig}_{\rm cas})\mathcal{F}^{\rm sig}_{\rm dir} + g^{\rm sig}_{\rm cas}\mathcal{F}^{\rm sig}_{\rm cas}] + g^{\rm sig}_{\rm Dtag}\mathcal{F}_{\rm Dtag}\} \\
&+f^{\rm peak}[(1-g^{\rm sig}_{\rm Dtag})\mathcal{F}^{+}_{\rm dir} + g^{\rm sig}_{\rm Dtag}\mathcal{F}_{\rm Dtag}] \\
&+f^{\rm comb}\{(1-g^{\rm bkg}_{+}-g^{\rm bkg}_{\rm Dtag})[(1-g^{\rm bkg}_{\rm cas}-g^{\rm bkg}_{\rm cas,2})\mathcal{F}^{\rm bkg}_{\rm dir} \\
&+g^{\rm bkg}_{\rm cas}\mathcal{F}^{\rm bkg}_{\rm cas} + g^{\rm bkg}_{\rm cas,2}\mathcal{F}^{\rm bkg}_{\rm cas,2}] + g^{\rm bkg}_{+}\mathcal{F}^{\rm bkg}_{+} + g^{\rm bkg}_{\rm Dtag}\mathcal{F}_{\rm Dtag}\} \\
&+f^{\rm cont}\mathcal{F}^{\rm cont}
\end{aligned} \tag{14}$$

where g^i_j are generic fractions of the tagging category j in sample i and we assume the fractions of decay-side tagged events, determined from Monte Carlo simulation, to be equal in the signal and peaking background components.

A crucial point of this analysis is to determine particle detection asymmetries, that could in principle be degenerate with the CP asymmetry. A method commonly used for determining detection asymmetries in time-dependent analyses is to use tagged and untagged events reconstructed as B^0 or $\overline{B}^0$, to have four equations from which ε_{tag}, ε_{rec}, A_{rec} and A_{tag} are determined uniquely. This procedure, fully explained in Appendix of [7], is however appropriate when CP violation in mixing is assumed to be zero. Here we must employ a different approach. We parameterize the total number of expected events for each tagged and untagged category in a likelihood function, which contains a term coming from the shapes of the PDFs for tagged events, an extended term for the number of tagged events and an extended term for the number of untagged events. We show the procedure in full detail for signal events. The expected number of tagged events per category is obtained in a straightforward way by integrating Eqs. (9) and (10), while for untagged events:

$$N_{exp}(s_u) = N_{tot}\frac{1-s_u A_{rec}}{2}[1-\varepsilon_{tag}+s_u\varepsilon_{tag}A_{tag}x_d - s_u k(1-x_d)(1-\varepsilon_{tag})] \tag{15}$$

where N_{tot} is the total number of events (tagged and untagged), $x_d = 1/[1+(\tau_{B^0}\Delta m_d)^2]$ and $s_u = +1(-1)$ for B^0 ($\overline{B}^0$) untagged events.

The likelihood function to be maximized is of the form:

$$\ln L_{tot} = \ln L - \sum_{s_t,s_m}\ln L^{ext}(s_t,s_m) - \sum_{s_u}\ln L^{ext}(s_u), \tag{16}$$

where $\ln L^{ext}(i,(j)) = \ln(N^{i,(j)}_{obs}!) - N^{i,(j)}_{obs}\ln N^{i,(j)}_{exp} + N^{i,(j)}_{exp}$ are the extended terms for tagged and untagged events while $\ln L$ is the log-likelihood constructed starting from Eq. (14). This method reduces the correlation between CP mixing asymmetry and particle detection asymmetry, that nevertheless remains significant, as quoted in Sec. 6.

5 FITS OF SIMULATED SAMPLES

Several tests were performed on simulated events to verify that the fit determines the free parameters k, A_{rec} and A_{tag} correctly. First, fits to the various components of the Monte Carlo sample and to the total $B\overline{B}$ sample were performed to check for the presence of biases in the analysis technique. This Monte Carlo sample was generated with a value of k equal to 0. We summarize in Table 2 the result of these fits for side-band region (first column) and signal region (second column). τ_{B^0},

τ_{B^+} and Δm_d are fixed to the generated values in this procedure, while the normalizations of the various contributions are fixed to the values extracted from the M_ν^2 distribution.

The most notable parameters in Table 2 are the asymmetries k, A_{rec}, A_{tag}, $A_{rec}^{\rm bkg}$ and A'_{tag}. We find all to be compatible with 0, except $A_{rec}^{\rm bkg}$ and A'_{tag}. The source of $A_{rec}^{\rm bkg} \neq 0$ is random tracks reconstructed as soft pions in the combinatorial background. We do not use a control sample for estimating $A_{rec}^{\rm bkg}$ but we use the value found in the side-band fit; its possible variation from side-band to signal region is taken into account during systematic evaluation. From Monte Carlo studies, we find that the source of $A'_{tag} \neq 0$ is charged kaons from the unreconstructed $\overline{D}^0$ faking muons. We compare the asymmetry value found in the Monte Carlo sample (second column of Table 2) with the value calculated in a charged kaon control sample ($D^* \ \rightarrow \ D^0\pi$, $D^0 \rightarrow K\pi$ decays) from the integrated K^+ and K^- efficiencies over the tag lepton momentum spectrum. This is found to be compatible with the fitted value ($A'_{tag,CS} = (18.0 \pm 0.5)\%$). We then conclude that the asymmetry can be considered as entirely due to this source and we fix the value of A'_{tag} to the one found in the control sample. A similar procedure is then exploited in the data fit.

Other checks are performed using large numbers of toy experiments, each generated with statistics corresponding to the size of the data sample. A set of 120 toy experiments is used to test the validity of the uncertainty calculated by the minimization algorithm and to check that the final value of the negative-log-likelihood is compatible with the value found in the data. Other Monte Carlo samples are generated with values of k or A_{rec} or A_{tag} equal to ± 0.01 to check the feasibility of disentangling the asymmetries from one another. The fits show that this disentanglement is possible. Also, a CP asymmetry different from 0 is generated in the generic $B^0\overline{B}^0$ sample to verify the sensitivity of the fit to values of $k \neq 0$. We find $k = (8.9 \pm 2.9) \cdot 10^{-3}$ for a generated value of $10 \cdot 10^{-3}$ and $k = (-10.1 \pm 2.9) \cdot 10^{-3}$ for a generated value of $-10 \cdot 10^{-3}$.

6 FITS OF THE DATA SAMPLE

The same procedure used in Monte Carlo events is applied to the on-resonance data. We float the same set of parameters and we fix the others in the following way. The tagging efficiency ε_{tag} is determined from the number of tagged events divided by the total number of events: we find $\varepsilon_{tag} = (9.06 \pm 0.02)\%$. For continuum events we use parameters taken from the off-resonance fit. For combinatorial background, some parameters are floated, some are fixed from a previous side-band fit (see Table 2). For signal and peaking background, we take dilutions from Monte Carlo and we float most resolution parameters. For A'_{tag}, we approximate its value using the estimate from the control sample explained above, assuming the fraction of charged kaon mistagging is the same as in Monte Carlo (we tested this hypothesis, as described in Sec. 7). We obtain an asymmetry of $A'_{tag} = (7.6 \pm 0.8)\%$ from the control sample. τ_{B^0}, Δm_d and τ_{B^+} are fixed to their PDG values [14]; the former two are then floated to estimate the fit stability in data when these parameters are free.

The fit results are shown in Table 2 (third and fourth column); for the three signal asymmetry parameters we find the following correlation coefficients: $\rho(A_{tag}, A_{rec}) = 43.4\%$, $\rho(k, A_{rec}) = 50.2\%$, $\rho(k, A_{tag}) = 88.5\%$. Figs. 2 and 3 show the fitted PDFs for the subsamples equivalent to the four tag-mixing states; Pearson's test gives a χ^2 of 682 for 385 degrees of freedom. Fig. 4 shows the PDF asymmetry derived from the fit in Fig. 2 between mixed events with $s_t = 1$ and $s_t = -1$.

Table 2: Top: results of the fits to the $B\overline{B}$ Monte Carlo and for: side-band region (first column), signal region (second column). Results of the fits to the on-resonance sample for side-band region (third column), signal region (fourth column). We also report asymmetrical errors for some fundamental parameters. A horizontal line is used to separate signal from background parameters. Bottom: Continuum parameters determined from the total off-resonance sample: they are fixed in the nominal on-peak data fit.

Parameter	Side-band fit (MC)	Signal region fit (MC)	Side-band fit (data)	Signal region fit (data)
k	$(0.8 \pm 3.0)\cdot10^{-3}$	$(-1.6 \pm 1.7)\cdot10^{-3}$	$(-2.1 \pm 4.9)\cdot10^{-3}$	$(6.0 \pm 3.4)\cdot10^{-3}$ [+3.4, -3.5]
A_{rec}	-	$(0.02 \pm 0.06)\cdot10^{-3}$	-	$(1.0 \pm 1.5)\cdot10^{-3}$ [+1.5, -1.5]
A_{tag}	$(-0.2 \pm 2.4)\cdot10^{-3}$	$(0.3 \pm 1.1)\cdot10^{-3}$	$(-0.2 \pm 2.9)\cdot10^{-3}$	$(3.1 \pm 2.1)\cdot10^{-3}$ [+2.1, -2.1]
$b^{\rm dir}$	-	-0.049 ± 0.002	-	-0.044 ± 0.008
$s_n^{\rm dir}$	-	0.859 ± 0.007	-	1.15 ± 0.02
f_w	-	$(9.6 \pm 0.3)\%$	-	$(9.2 \pm 0.7)\%$
s_w	-	1.90 ± 0.03	-	1.90 (fixed)
s_o	-	(7.2 ± 0.5) ps	-	7.2 ps (fixed)
f_o	-	$(2.7 \pm 0.3)\cdot10^{-3}$	-	$2.7\cdot10^{-3}$ (fixed)
$w_{\rm dir}$	-	$(1.32 \pm 0.04)\%$	-	1.32% (fixed)
$\Delta w_{\rm dir}$	-	$(-3.2 \pm 7.8)\cdot10^{-4}$	-	$-3.2\cdot10^{-4}$ (fixed)
τ_{D_e}	(0.226 ± 0.009) ps	(0.267 ± 0.008) ps	(0.342 ± 0.015) ps	(0.321 ± 0.010) ps
$w_{\rm cas}$	-	$(20.8 \pm 2.4)\%$	-	20.8% (fixed)
$\Delta w_{\rm cas}$	-	$(1.0 \pm 0.4)\%$	-	1.0% (fixed)
$b_n^{\rm cas}$	-	-0.33 ± 0.04	-	-0.28 ± 0.09
$b_w^{\rm cas}$	-	-2.4 ± 0.3	-	-2.4 (fixed)
A'_{tag}	-	$(18.9 \pm 1.0)\%$	-	7.6% (fixed, see text)
$D_{\rm Dtag}$	-	$(83.7 \pm 2.0)\%$	-	83.7 (fixed)
$g_{\rm cas}^{\rm sig}$	-	$(6.67 \pm 0.20)\%$	-	$(5.0 \pm 0.5)\%$
$g_{\rm Dtag}^{\rm sig}$	-	5.62% (fixed)	-	5.62% (fixed)
D_+	$(80.6 \pm 0.8)\%$	$(90.1 \pm 2.5)\%$	$(83.2 \pm 1.8)\%$	$(83.4 \pm 4.2)\%$
$\tau_{B^0}^{\rm bkg}$	(1.469 ± 0.017) ps	(1.28 ± 0.04) ps	(1.51 ± 0.03) ps	(1.53 ± 0.02) ps
$\Delta m_d^{\rm bkg}$	(0.479 ± 0.007) ps^{-1}	(0.37 ± 0.04) ps^{-1}	(0.506 ± 0.010) ps^{-1}	(0.586 ± 0.010) ps^{-1}
$A_{rec}^{\rm bkg}$	$(3.9 \pm 2.3)\cdot10^{-3}$	$3.9\cdot10^{-3}$ (fixed)	$(9.7 \pm 2.9)\cdot10^{-3}$	$9.7\cdot10^{-3}$ (fixed)
$w_{\rm dir}^{\rm bkg}$	$(1.19 \pm 0.07)\%$	1.19% (fixed)	1.19% (fixed)	1.19% (fixed)
$\Delta w_{\rm dir}^{\rm bkg}$	$(1.4 \pm 0.9)\cdot10^{-3}$	$1.4\cdot10^{-3}$ (fixed)	$1.4\cdot10^{-3}$ (fixed)	$1.4\cdot10^{-3}$ (fixed)
$b_{\rm bkg}^{\rm dir}$	0.071 ± 0.036	-0.034 ± 0.030	0.013 ± 0.006	-0.056 ± 0.008
$s_{n,{\rm bkg}}^{\rm dir}$	0.837 ± 0.006	0.837 (fixed)	0.850 ± 0.011	0.850 (fixed)
$f_w^{\rm bkg}$	$(7.6 \pm 0.5)\%$	$(6.1 \pm 0.5)\%$	$(12.7 \pm 0.8)\%$	$(7.4 \pm 1.5)\%$
$x_d^{\rm bkg}$	0.205 ± 0.009	0.205 (fixed)	0.420 ± 0.012	0.420 (fixed)
$w_{\rm cas}^{\rm bkg}$	$(18.7 \pm 0.6)\%$	18.7% (fixed)	18.7% (fixed)	18.7% (fixed)
$\Delta w_{\rm cas}^{\rm bkg}$	0.017 ± 0.006	0.017 (fixed)	0.017 (fixed)	0.017 (fixed)
$b_{n,{\rm bkg}}^{\rm cas}$	-0.02 ± 0.06	-0.02 (fixed)	-0.13 ± 0.08	-0.13 (fixed)
$b_{n,{\rm bkg}}^{\rm cas,2}$	0.02 ± 0.08	0.02 (fixed)	0.15 ± 0.11	0.15 (fixed)
$g_{\rm Dtag}^{\rm bkg}$	$(13.0 \pm 0.2)\%$	$(9.2 \pm 0.8)\%$	$(8.5 \pm 0.5)\%$	$(6.1 \pm 0.8)\%$
$g_+^{\rm bkg}$	$(40.7 \pm 0.3)\%$	$(37.1 \pm 0.2)\%$	$(33.7 \pm 0.5)\%$	$(31.9 \pm 0.3)\%$

Parameter	Value from off-peak fit
$\tau_{\rm cont}$	(0.62 ± 0.03) ps
$A_{rec}^{\rm cont}$	$(6.4 \pm 2.1)\%$
$A_{tag}^{\rm cont}$	$(3.9 \pm 2.9)\%$
$D_{\rm cont}$	$(47.8 \pm 1.6)\%$

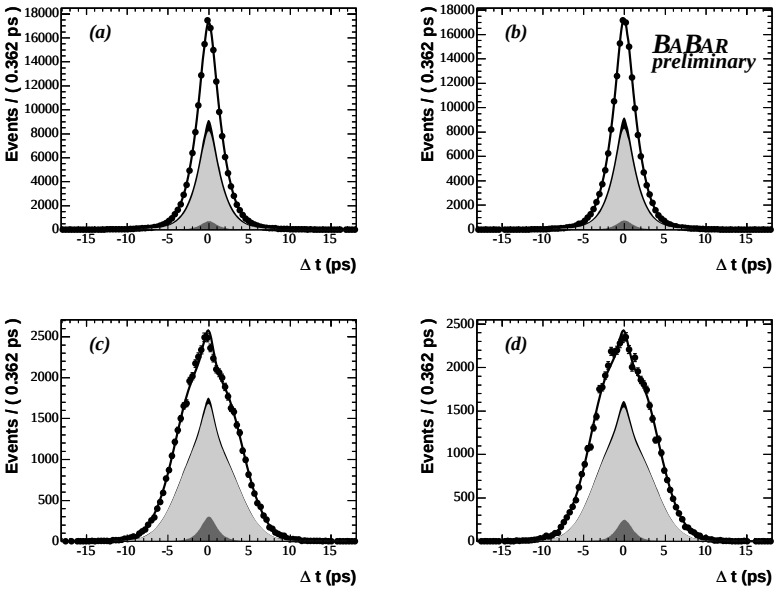

Figure 2: Fit to the Δt distributions for the on-resonance data samples in linear scale. Letters indicate the different samples: (a) Unmixed positive ($s_m = 1, s_t = 1$), (b) Unmixed negative ($s_m = 1, s_t = -1$), (c) Mixed positive ($s_m = -1, s_t = 1$), (d) Mixed negative ($s_m = -1, s_t = -1$). The following fitted contributions are shown in the fit: continuum (dark grey), combinatorial (light grey), $B^{\pm}$ peaking (black), signal (white).

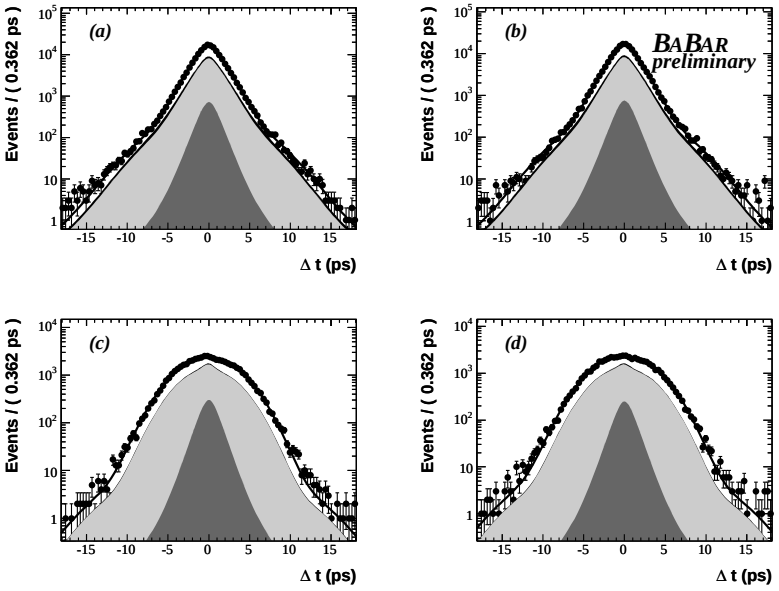

Figure 3: Same as Fig. 2 in logarithmic scale.

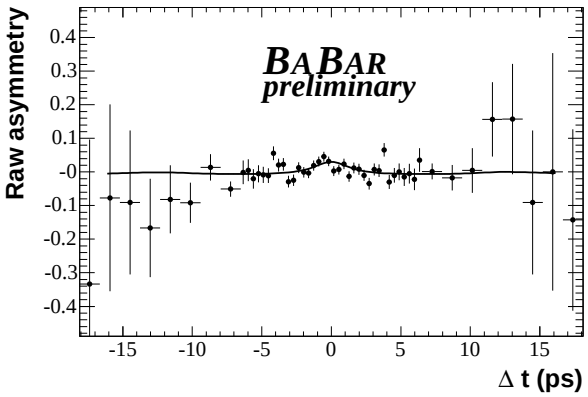

Figure 4: Raw asymmetry between mixed positive ($s_m = -1, s_t = 1$) and mixed negative ($s_m = -1, s_t = -1$) events with the PDF asymmetry derived from the fit in Fig. 2 superimposed. The asymmetry at low values of $|\Delta t|$ corresponds to the kaon-mistag contribution in decay-side tagged events (see text).

7 SYSTEMATIC STUDIES

We consider the following sources of systematic uncertainties.

For the reconstruction asymmetry for combinatorial background events, we repeat the fit in the first column of Table 2 for combinatorial Monte Carlo events in the signal region, finding $A_{rec}^{\rm bkg} = (6.5 \pm 2.1) \cdot 10^{-3}$. The difference between this result and the one in the sideband ($= 2.6 \cdot 10^{-3}$) is applied to the reconstruction asymmetry in data and the fit is re-done to estimate the impact on k.

We vary the continuum reconstruction and tagging asymmetries by $\pm 1\sigma$, where the standard deviations are taken from the fit to the off-peak events. The variations in k are averaged and added in quadrature to give the systematic uncertainty.

We perform a fit in which the asymmetry A'_{tag} is free rather than fixed from a control sample: we obtain $A'_{tag} = (4.0 \pm 3.8)\%$ which is compatible with the assumption that the fraction of kaon mistagging is the same as in Monte Carlo, but the uncertainties are large because of the high correlation between A_{tag} and A'_{tag}. The resulting variation in k is taken as a systematic uncertainty.

We vary the sample fractions by $\pm 1\sigma$, where the statistical errors are taken from the M_ν^2 data fits, both to tagged and untagged events separately. Moreover, for B^0 and $\overline{B}^0$ untagged events, we move the two central values in opposite directions in order to consider the maximum asymmetry that could be generated by the fit uncertainty. Similarly, we vary the fractions of their correlated systematic uncertainties simultaneously for tagged and untagged events. Continuum fractions are varied by the uncertainty in the on/off-resonance luminosity ratio, which we take as 1.3% from [10].

For the analysis technique, we determine the mean of $k_{\rm fit} - k_{\rm gen}$ in the Monte Carlo tests we performed and we correct the result on data accordingly; the full size of the correction ($5.5 \cdot 10^{-4}$) is taken as a systematic uncertainty.

We let τ_{B^0} and Δm_d float in the data fit, obtaining $\tau_{B^0} = (1.551 \pm 0.012)$ ps and $\Delta m_d = (0.475 \pm 0.019)$ ps^{-1} which are in good agreement with the world averages [14], considering a known bias on Δm_d caused by the partial reconstruction technique [15].

Most mistag parameters for the various samples are fixed in the data fit. When omitting decay-side tagged events, we can assume mistagging is almost entirely due to charged pions. Using inclusive pion control samples, we notice that for both negative and positive pions, the relative difference between data and Monte Carlo is smaller than 10%. We conservatively vary the mistags of 10% and quote the variations of k as a systematic uncertainty.

Also some parameters of the resolution are fixed, namely the fraction and width of the "outlier" Gaussian and the width of the "wide" Gaussian are fixed. For the former, we repeat the fit setting $f_o = 0$ (2-Gaussian resolution only), the latter is varied by 30% conservatively.

All other parameters that are fixed from the sidebands or from the off-resonance fit are varied by their statistical errors to estimate corresponding systematic uncertainties.

All the variations in k are summed in quadrature. The effect on the parameter k for all these sources, as well as the total uncertainty is summarized in Table 3.

Table 3: Sources of systematic uncertainty for the $|q/p|$ measurement.

Source	Syst. error ($\cdot 10^{-3}$)
Reconstruction asymmetry for combinatorial background	1.1
Asymmetries for continuum	1.0
Tagging asymmetry for decay-side tagged events	0.2
M^2_ν fractions	1.0
Likelihood fit bias	0.6
Physical parameter fixing	0.5
Mistag parameters	0.0
Resolution function	0.3
Sideband-fixed parameters	0.5
Total	2.0

8 RESULTS

From the fit performed on the on-resonance data sample we measure:

$$|q/p| - 1 = (6.5 \pm 3.4(\text{stat.}) \pm 2.0(\text{syst.})) \cdot 10^{-3}$$

which relates to CP violation in mixing.

To facilitate comparison with other measurements and formalisms, we also express our result in two other commonly used notations. The parameter A_{SL} defined in Eq. (4) is found to be:

$$A_{SL} = \frac{1 - |q/p|^4}{1 + |q/p|^4} = (-13.0 \pm 6.8(\text{stat.}) \pm 4.0(\text{syst.})) \cdot 10^{-3}$$

or, using the ε_B parameter and the relation $q/p = (1 - \varepsilon_B)/(1 + \varepsilon_B)$:

$$\frac{\text{Re}\varepsilon_B}{1 + |\varepsilon_B|^2} \simeq \frac{A_{SL}}{4} = (-3.2 \pm 1.7(\text{stat.}) \pm 1.0(\text{syst.})) \cdot 10^{-3}$$

9 SUMMARY

We have presented a determination of the parameter $|q/p|$, that is a measurement of CP violation in $B^0\overline{B}^0$ mixing, using a fit to Δt, the time difference between the two B decays. One of the B mesons is partially reconstructed in the semileptonic channel $D^{*-}\ell^+\nu_\ell$, i.e. only the lepton and the soft pion from $D^{*-} \to \overline{D}^0\pi^-$ decay are reconstructed, while the flavor of the other B is determined by means of lepton tagging. We use a luminosity of 200.8 fb^{-1} collected by the *BABAR* detector in the period 1999-2004, and obtain the preliminary result:

$$|q/p| - 1 = (6.5 \pm 3.4(\text{stat.}) \pm 2.0(\text{syst.})) \cdot 10^{-3}\,.$$

This result is compatible with the current world average, and the magnitude of its error is comparable to those of the most recent other measurements [5, 6]. The corresponding central confidence interval at 95% C.L. for $|q/p|$ is $[1.0012 - 1.0142]$.

10 ACKNOWLEDGMENTS

We are grateful for the extraordinary contributions of our PEP-II colleagues in achieving the excellent luminosity and machine conditions that have made this work possible. The success of this project also relies critically on the expertise and dedication of the computing organizations that support *BABAR*. The collaborating institutions wish to thank SLAC for its support and the kind hospitality extended to them. This work is supported by the US Department of Energy and National Science Foundation, the Natural Sciences and Engineering Research Council (Canada), Institute of High Energy Physics (China), the Commissariat à l'Energie Atomique and Institut National de Physique Nucléaire et de Physique des Particules (France), the Bundesministerium für Bildung und Forschung and Deutsche Forschungsgemeinschaft (Germany), the Istituto Nazionale di Fisica Nucleare (Italy), the Foundation for Fundamental Research on Matter (The Netherlands), the Research Council of Norway, the Ministry of Science and Technology of the Russian Federation, and the Particle Physics and Astronomy Research Council (United Kingdom). Individuals have received support from the Marie-Curie IEF program (European Union) and the A. P. Sloan Foundation.

References

[1] M. Ciuchini *et al.*, JHEP **0308**, 031 (2002).

[2] M. Beneke *et al.*, Phys. Lett. **B 576**, 173 (2003).

[3] S. Laplace *et al.*, Phys. Rev. **D**65, 094040 (2002).

[4] M. Kobayashi and T. Maskawa, Prog. Theor. Phys. **49**, 652 (1973).

[5] K. Abe *et al.*, The BELLE Collaboration, Phys. Rev. **D**73, 112002 (2006).

[6] B. Aubert *et al.*, The *BABAR* Collaboration, Phys. Rev. Lett. **96**, 251802 (2006).

[7] B. Aubert *et al.*, The *BABAR* Collaboration, Phys. Rev. **D**70, 012007 (2004).

[8] http://www-d0.fnal.gov/Run2Physics/WWW/results/prelim/B/B29/B29.pdf.

[9] M. Bona *et al.*, The UT*fit* Collaboration, hep-ph/0605213.

[10] The *BABAR* Collaboration, B. Aubert *et al.*, Nucl. Instrum. Methods **A479**, 1-116 (2002).

[11] G. C. Fox and S. Wolfram, Phys. Rev. Lett. **41**, 1581 (1978).

[12] Unless specified, all four-momenta are measured in the $\Upsilon(4S)$ rest frame.

[13] With $m \equiv M_\nu^2$, we define $\mathcal{B}(m) = [(m - m_0)^{a_1} + c(m - m_0)^{a_2}]e^{-b(m-m_0)}$.

[14] Particle Data Group, S. Eidelman *et al.*, Phys. Lett. **B592**, 1 (2004).

[15] B. Aubert *et al.*, The *BABAR* Collaboration, Phys. Rev. **D**73, 012004 (2006).